Stress-Relaxation Behavior of Natural Rubber/Polystyrene and Natural Rubber/Polystyrene/Natural Rubber-*graft*-Polystyrene Blends

R. Asaletha,[1] P. Bindu,[2] Indose Aravind,[2] A. P. Meera,[2] S. V. Valsaraj,[2] Weimin Yang,[3] Sabu Thomas[2]

[1]*Cochin University College of Engineering, Kuttanadu, Pulinkunnu Post Office, Allappey, Kerala, India*
[2]*School of Chemical Sciences, Mahatma Gandhi University, Priyadarshini Hills Post Office, Kottayam, Kerala 686560, India*
[3]*Department of International Exchanges & Cooperation, Beijing University of Chemical Technology, Bei San Huan East Road 15#, Chaoyang District, Beijing, China*

Received 15 September 2006; accepted 11 July 2007
DOI 10.1002/app.27395
Published online 18 January 2008 in Wiley InterScience (www.interscience.wiley.com).

ABSTRACT: We studied the stress-relaxation behavior of natural rubber (NR)/polystyrene (PS) blends in tension. The effects of strain level, composition, compatibilizer loading, and aging on the stress-relaxation behavior were investigated in detail. The dispersed/matrix phase morphology always showed a two-stage mechanism. On the other hand, the cocontinuos morphology showed a single-stage mechanism. The addition of a compatibilizer (NR-*g*-PS) into 50/50 blends changed the blend morphology to a matrix/dispersed phase structure. As a result, a two-step relaxation mechanism was found in the compatibilized blends. A three-stage mechanism was observed at very high loadings of the compatibilizer (above the critical micelle concentration), where the compatibilizer formed micelles in the continuous phase. The aged samples showed a two-stage relaxation mechanism. The rate of relaxation increased with strain levels. The aging produced interesting effects on the relaxation pattern. The rate of relaxation increased with temperature due to the degradation of the samples. © 2008 Wiley Periodicals, Inc. J Appl Polym Sci 108: 904–913, 2008

Key words: blends; compatibility; polystyrene; rubber; stress

INTRODUCTION

Polymer blends have received increasing attention in the field of polymer science and industry. The growth of the use of polymer blends has mainly been due to their ability to combine the properties of their phases in a unique product. The final properties of polymer blends are directly related to their microstructure and morphology. However, most polymer blends are incompatible, which results in materials with coarse morphology, weak adhesion among phases, and poor mechanical properties. These blends exhibit many interesting behaviors, including enhanced elasticity at small strains, drop-size hysteresis, enhanced shear thinning, and stress-relaxation curves whose shapes are sensitive to deformation history. These behaviors are directly related to changes in the microstructure, which result from phase deformation, coalescence, retraction, and different types of breakup. These phenomena have been reviewed,[1] together with models that describe them. Furthermore, polymer blends often operate under conditions where factors such as fatigue, creep, stress relaxation, and chemical attack are significant. Such materials can fail by progressive degradation, which results in hardening, softening, set, crack growth, or fracture.[2]

Thermoplastic elastomers (TPEs) can be obtained by the blending of thermoplastics and rubbers.[3–5] The resulting materials combine the excellent processing characteristics of thermoplastics and the elastic properties of rubbers. Although the preparation of TPEs through blending is an easy method, most TPE blends are immiscible and incompatible. As a result, these blends often exhibit poor mechanical properties due to the poor adhesion between the phases. This problem can be solved by the addition of suitable copolymers that act as compatibilizers. Asaletha et al.[5] prepared TPEs from blends of natural rubber (NR) and polystyrene (PS). A graft copolymer of NR and PS (NR-*g*-PS) was found to increase the compatibility of the system.

Correspondence to: W. Yang (yangwm@mail.buct.edu.cn) or S. Thomas (sabut552001@yahoo.com or sabut@sancharnet.in).
Contract grant sponsor: Council of Scientific and Industrial Research (to R.A.).
Contract grant sponsor: Department of Science and Technology (to R.A.).

The stress relaxation of multiphase polymer blend systems has received a lot of attention in recent years. Mewis et al.[6] reported on the transient stress response after the inception of flow in immiscible blends using nearly Newtonian components. The contributions from the components and from the interface to the total stress were determined experimentally by means of relaxation measurements. In this manner, the different contributions to the stress could be compared separately with model predictions. For the contribution of the components, one normally uses mixing rules that do not take into account the morphology of the blend. As expected, a slight morphology effect can be detected. The stress contributions from the interface are calculated combining the Doi–Ohta[7] approach with different models that describe the droplet deformation. For flows at small capillary numbers, the Maffettone–Minale[8] model leads to accurate stress predictions. Cristini et al.[9] presented a numerical investigation of transient stresses in immiscible blends of Newtonian components. The simulations were based on the deformation of a single droplet immersed in an infinite matrix subjected to flow. This study aimed to demonstrate the predictive power of the simulations for rheological properties in dilute blends for both subcritical and supercritical startup flows. Brostow et al.[10] reported the results of the determination of the stress relaxation of polypropylene, a polymer liquid crystal, and two binary blends of these components. For each material, they performed experiments at several temperatures and combined the results to achieve long-term predictions for a single temperature. The relation between the shift factor and the reduced volume was used to predict the long-term behavior of the materials from a minimum (at least two sets) of data. To describe the dynamics of the linear polymer in monodisperse melts, Koga et al.[11] presented a reaction-diffusion type equation that contained contributions from reptation and contour-length fluctuation on the basis of the tube model. The relaxation function calculated from this equation was in good agreement with the experimental results of the dielectric relaxation function and also gave the stress-relaxation function in binary blends by use of a semi-empirical scheme called *double reptation*. The advection term was added to this equation to predict the nonlinear rheological properties of steady shear. The calculated shear stress and the first normal stress difference at steady state agreed well with the measurements. Stress prediction for immiscible polymer blends under flow has long been investigated. From an industrial point of view, stress prediction is important for finding better process conditions and for controlling blend morphology. However, stress prediction is still very difficult because the excess stress due to the anisotropy of the interface is directly related to the evolution of the interface shape under flow. The excess shear stress after the application of large-step strains in polymer blends is calculated from the observed shapes of deformed droplets in the immiscible matrix[12] on the basis of the Doie–Ohta[7] expression for the interface contribution to the stress. The calculation is made for droplet shapes of flat ellipsoids, rods with end caps, dumbbells, and ellipsoids of revolution. The predicted excess relaxation modulus agreed very well with experimental data normalized per one droplet with the volume-average radius for a polyisobutylene/poly(dimethyl siloxane) blend with a narrow distribution of droplet size. Especially, slow stress relaxation in the intermediate stage and faster relaxation thereafter predicted from the rodlike and dumbbell shapes were consistent with the experimental data. For a blend of a hydroxypropylcellulose solution and poly(dimethyl siloxane) with a broad distribution of droplet size, the predicted excess relaxation modulus agreed reasonably well with experimental data when the size distribution was taken into account.

In this article, we report on the stress-relaxation behavior of NR/PS blends in tension with and without the addition of a compatibilizer, that is, NR-*g*-PS. The relaxation behavior was also studied with special reference to the effects of strain level, blend ratio, and aging. Attempts were made to correlate the morphology with the relaxation process. To the best of our knowledge, to date, no studies have been made on the stress relaxation of NR/PS blends in the presence and absence of compatibilizers, although these blends find applications in many dynamic fields.

EXPERIMENTAL

Materials

PS was supplied by PolyChem, Ltd. (Bombay, India). NR (ISNR-5) was obtained from the Rubber Research Institute of India (Kottayam). The characteristics of the materials used are given in Table I.

Preparation of the graft copolymer

The graft copolymer of NR and PS (NR-*g*-PS) was prepared by the polymerization of styrene in rubber latex with ^{60}Co γ-radiation as the initiator.[13] Styrene monomer was made into an emulsion, which was then mixed with NR latex of known dry rubber content. The dose rate was 0.1166 Mrad/h. The free homopolymers NR and PS were removed from the crude sample by Soxhlet extraction with petroleum ether and methyl ethyl ketone, respectively.

TABLE I
Characteristics of the Materials Used

Material	Density (g/cm^3)	Solubility parameter $(cal/cm^3)^{1/2}$	Number-average molecular weight
NR	0.90	7.75	7.79×10^5
PS	1.04	8.56	3.51×10^5
$CHCl_3$	—	9.3	—
CCl_4	—	8.6	—
C_6H_6	—	9.2	—

Graft copolymer characterization

The graft copolymer (NR-*g*-PS) was characterized by Fourier transform infrared (FTIR) and ^{1}H-NMR spectroscopies and gravimetric methods. The grafting efficiency and percentage of PS grafted were 49 and 20%, respectively. This was estimated by gravimetric analysis, as reported earlier.[14]

The FTIR spectrum (Fig. 1) showed peaks at 3026 and 2855 cm^{-1}, which corresponded to aromatic C—H stretching in PS. Peaks at 1601 and 1541 cm^{-1} corresponded to the C=C stretching of the aromatic ring of PS. The peaks observed at 1452 and 1375 cm^{-1} indicated the presence of aliphatic C—H stretching in NR.

The ^{1}H-NMR spectrum obtained at 90 MHz (Fig. 2) showed chemical shifts at 1–2, 4.6–4.8, and 6.6 ppm corresponding to alkyl protons of NR and vinyl and aromatic protons of PS, respectively.

Blend preparation

NR and PS were blended together in a common solvent, chloroform (a 5% solution was made for casting). Different compositions of the blends (40/60, 50/50, and 60/40) were made with and without the addition of the graft copolymer. NR, PS, and the graft copolymer were mixed in chloroform. The mixture was kept overnight and then stirred for 8 h with a magnetic stirrer. Films were cast on a glass plate and dried in a vacuum oven at 80°C for 48 h and then at 120°C for another 4 h.

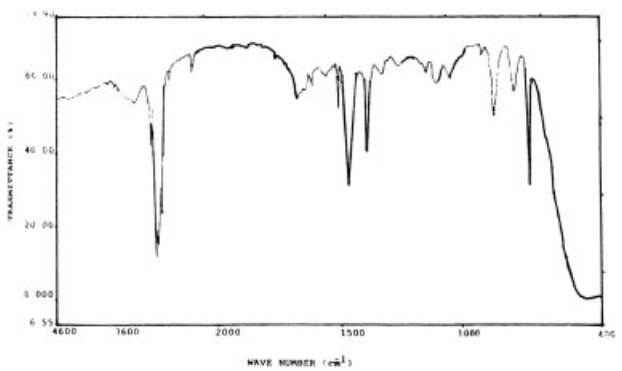

Figure 1 FTIR spectrum of the graft copolymer.

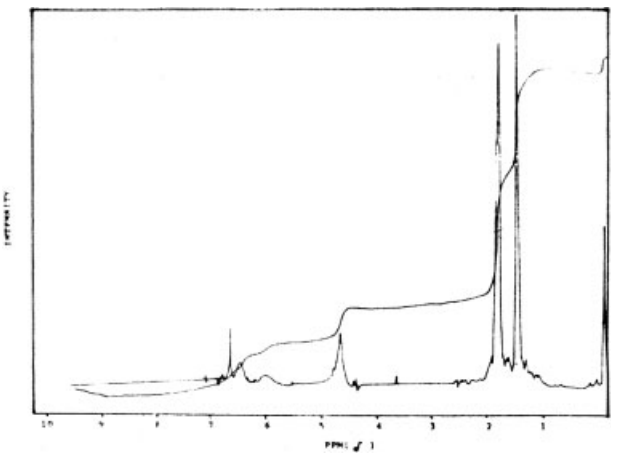

Figure 2 ^{1}H-NMR spectrum of the graft copolymer.

Stress relaxation

Stress-relaxation measurements were carried out in a Zwick universal testing machine (model 1474) with dumbbell-shaped test samples (dimensions as per ASTM D 412). The samples were pulled to the desired strain level at a strain rate of approximately 0.061 s^{-1}, and the decay in stress as a function of time was recorded. The experiments were carried out at room temperature (28°C). To study the effect of temperature, the samples were aged at 50 and 70°C for 4 days. The details of the different samples studied are given in Table II.

RESULTS AND DISCUSSION

Effect of the strain level

Linear plots of (σ_t/σ_0) versus log t of 60/40 NR/PS blends at different strain levels (50, 100, and 150%) are given in Figure 3, where σ_t is the stress at time t and σ_0 is the stress at $t = 0$. In all cases, the rate at

TABLE II
Details of the Samples

Sample	NR (wt %)	PS (wt %)	NR-*g*-PS (wt %)
A	40	60	—
B	50	50	—
C	60	40	—
D	50	50	1.5
E	50	50	3
F	50	50	4.5
G	50	50	—
H	50	50	—
I	60	40	—
J	60	40	—

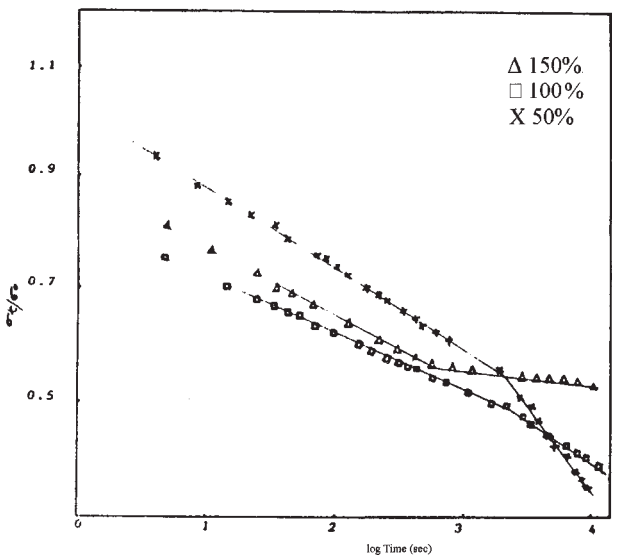

Figure 3 Effect of the strain level on the stress-relaxation pattern of the 60/40 NR/PS blend: (△) 150, (□) 100, and (×) 50%.

which the initial strain was attained was kept constant in all samples. The relaxation patterns of the samples were studied at different strains. There was only marginal variation in the initial rate of relaxation at all extensions. In all cases, the experimental points fell on two intersecting straight lines. This clearly indicated the two-phase structure of the blend. Two different straight lines will intersect at a point at which the relaxation mechanism changes from one mode to another. The time corresponding to this point is known as the *crossover time*. The values of crossover time were 1819, 622, and 2411 s for samples, C, I, and J, respectively. The slopes and intercepts of the two straight lines are given in Table III; these values were obtained by the linear regression analysis method. The difference in the values of the slopes and intercepts indicated that the mechanism of relaxation operated in two ways; one operated at shorter times, and another was prominent at the later stages of relaxation. The initial slope (i.e., relaxation rate) was nearly the same for all three strain levels. The slope and location of the second process depended on strain level. As the strain level decreased, the rate of relaxation in the second step increased. We calculated the contribution by the earlier process of relaxation, as reported by Mackenzie and Scanlan,[15] by dividing the differences of the two intercepts by the intercept of the first line at t = 1 s. As shown in Table III, as the strain level increased from 50% (sample J) to 150% (sample C); the contribution of the early process increased from 13.1 to 26.9% in the case of the noncompatibilized blend, and this was due to the high interfacial tension across the phase boundaries.

Effect of the composition

Figure 4 shows the stress-relaxation curves of different NR/PS blends of varying composition. In the case of the 50/50 blend, the experimental points fell on a single straight line, whereas in the other two cases (i.e., the 40/60 and 60/40 NR/PS blends), the experimental points fell on two intersecting straight lines, which indicated that the relaxation process followed two different mechanisms. In the case of the 40/60 NR/PS blend, NR was the dispersed phase, and PS formed the continuous phase. In the case of sample C (60/40 NR/PS blend), the reverse was true, and hence, the relaxation due to NR increased. As shown in Figure 2, the behavior of the 50/50 blend was different from the others. The relative stress decay was found to be a linear function of log t over the timescale studied. This indicated a single relaxation mechanism for the 50/50 blend, unlike the 60/40 and 40/60 blends. The difference in behavior could be understood from the morphology of the blend.

TABLE III
Results of the Stress-Relaxation Measurements

Sample	Slope (−ve)			Intercept			Contribution to the initial mechanism (%)	Crossover time (s)
	Initial	Intermediate	Final	Initial	Intermediate	Final		
A	0.0979	—	0.0572	0.9893	—	0.8655	12.5	762
B	0.0978	—	—	0.9937	—	—	—	—
C	0.1285	—	0.2253	1.0126	—	1.2858	26.9	1819
D	0.1147	—	0.0367	0.9316	—	0.6789	27.1	1698
E	0.0943	—	0.1035	0.9458	—	0.9650	20	2411
F	0.1182	0.8089	0.0989	0.9403	3.1842	0.7043	25.1	1718 (3383[a])
G	0.1191	—	0.0671	0.9412	—	0.8128	42.9	87
H	0.9698	—	900641	0.0997	—	0.0569	13.6	171
I	0.1086	—	0.0725	0.9437	—	0.8193	—	622
J	0.1200	—	0.1865	0.9318	—	—	13.1	2411

[a] Second crossover time.

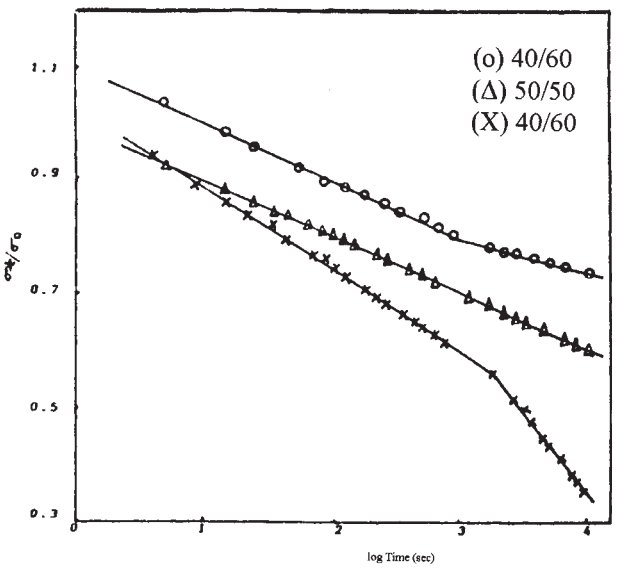

Figure 4 Effect of the composition on the stress-relaxation pattern of different NR/PS blends at a strain level of 150%: (○) 40/60, (△) 50/50, and (×) 40/60 NR/PS blends.

Figure 5 shows the morphologies of the NR/PS blends as a function of composition. Figure 5(a,c) represents the 40/60 and 60/40 NR/PS blends, respectively, where NR and PS formed the dispersed phase. In Figure 5(a), the dispersed rubber domain size is bigger than the dispersed plastic domains shown in Figure 5(c), and this was due to the coalescence of the rubber domains (Table IV). Because of the low viscosity of the PS phase as compared to NR, the coalescence of the NR domains were favored. For the 50/50 NR/PS blend [Fig. 5(b)], the components formed a cocontinuous morphology, and this accounted for the single-phase relaxation mechanism shown by the 50/50 NR/PS blend. Because the interfacial interaction was very high in the 50/50 blend due to the interpenetration of the phases, the system showed a single-stage relaxation. Also, the 50/50 NR/PS blend showed a partial cocontinuous morphology; that is, both dispersed and cocontinuous phases existed. In this case, the average domain size was measured on the basis of the dispersed phases present.

The stress-relaxation rate was analyzed by measurement of the slope and intercept of the relaxation curve. The slope, intercept, crossover time, and contribution to initial mechanism for different NR/PS blends were calculated as explained earlier and are given in Table III. As shown in Table III, the rate of stress relaxation was highest in the 60/40 NR/PS blend. The relaxation rate decreased as the amount of NR decreased from the 60/40 NR/PS blend to the 40/60 NR/PS blend because the overall relaxation

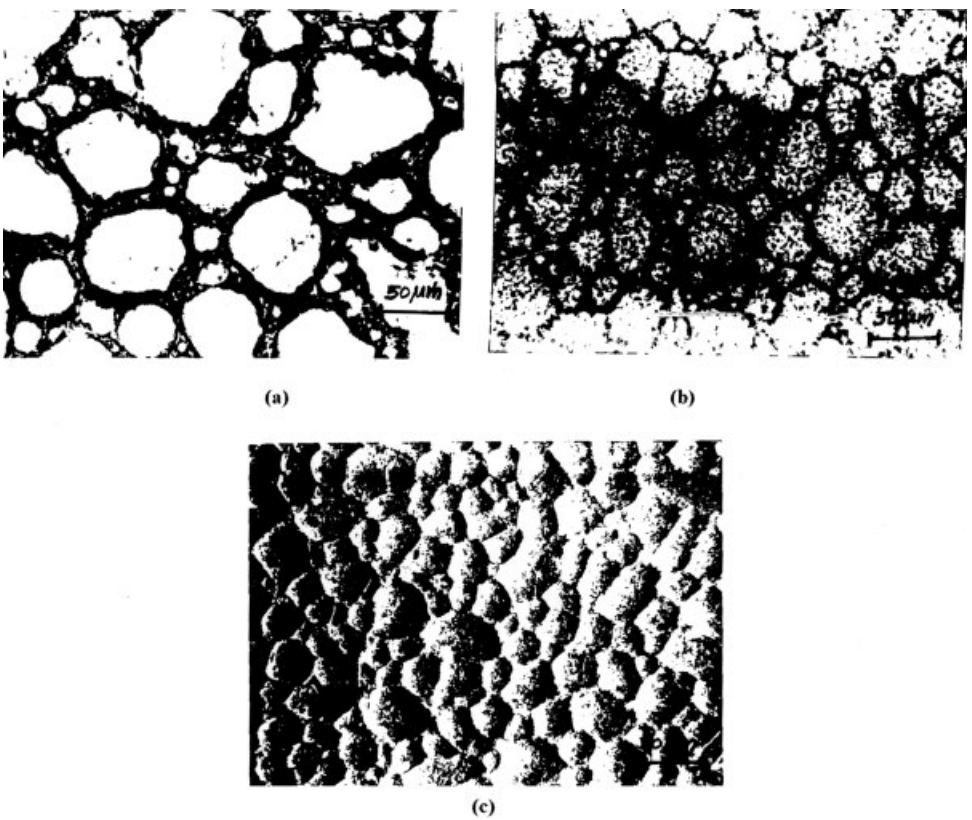

Figure 5 Optical micrographs of the (a) 40/60, (b) 50/50 and (c) 60/40 NR/PS blends.

TABLE IV
PDI Values of Different NR/PS Blends

Sample	Polydispersity index	Average domain diameter (μm)
40/60	1.24	17.14
50/50	1.14	14.11
60/40	1.09	13.45

process depended on the amount and domain size distribution of NR. This was further supported by the polydispersity index (PDI) values, which are given in Table IV. The 60/40 NR/PS blend possessed the minimum value of PDI, and hence, it exhibited the highest relaxation rate. As the PDI value increased from the 60/40 NR/PS blend to the 40/60 NR/PS blend, the relaxation rate decreased. The crossover time changed from 762 to 1819 s as the matrix phase changed from PS to NR. This was due to the difference in the concentration of NR, which contributed largely to the relaxation process. As shown in Table III, the contribution to the initial mechanism changed from 12.5 to 26.9% as the continuous phase changed from PS to NR.

Effect of the compatibilizer loading

Figure 6 shows the stress-relaxation curves of the 50/50 NR/PS blends with varying amounts of the compatibilizer, that is, NR-*g*-PS copolymer. The relaxation pattern of the compatibilized blend was different from that of the noncompatibilized one. In the case of the noncompatibilized blend, the experimental points fell on a single straight line, which indicated that the process of relaxation operated by a single mechanism. For the compatibilized blends (samples D and E), the experimental points fell on two intersecting straight lines. This was because the partially cocontinuous morphology was transformed into a well-defined matrix/dispersed morphology upon compatibilization. Compared to the noncompatibilized blend, the compatibilized blends showed an increase in the rate of relaxation because the compatibilizer added was located at the blend interface, which enhanced the interaction between the two phases. In the case of the compatibilized blends, compared to the noncompatibilized blends, the interfacial free energy was lower, which enhanced the stress-relaxation process. In sample F, that is, the 50/50 NR/PS blend with 4.5% compatibilizer, the graft copolymer formed micelles in the continuous phase, and thereby, a different pattern of relaxation was observed. A three-stage mechanism was shown at this loading of compatibilizer. The rate of relaxation was higher compared to that in blends with lower graft loadings. In the case of the compatibilized blends (samples D, E, and F), the contribution to the early process was nearly constant because of enhanced interfacial adhesion between the blend components. The first crossover time in the case of sample F was lower (1718 s) compared to that in sample E (2411 s) and was related to the formation of undesirable micelles. The second crossover time in this case was higher (3383 s) and led to a third mechanism, which was due to micelle formation in addition to the blend components.

Let us now examine the morphology of the blends in detail and try to relate the stress-relaxation process with the morphology. The NR/PS blends were completely immiscible. The compatibility of the system was improved by the addition of the compatibilizer, that is, the graft copolymer of NR and PS (NR-*g*-PS). The size of the dispersed PS domains decreased with increasing percentage of the graft copolymer. We examined the morphology of 40/60, 50/50, and 60/40 NR/PS blends. Figure 7 shows the optical microphotographs of 50/50 NR/PS blends with and without the addition of the copolymer. This blend had a partially cocontinuous morphology; that is, both the dispersed and continuous phases of NR could be seen in the continuous PS matrix. We measured the number-average domain size by noting the diameter of a large number of domains at random in each blend system. The average domain size decreased with increasing concentration of the compatibilizer and finally leveled off at higher concentrations (Fig. 8). This leveling off point was considered the so-called apparent critical micelle concentration (cmc), that is, the concentration of the copolymer at which micelles were formed. This sort

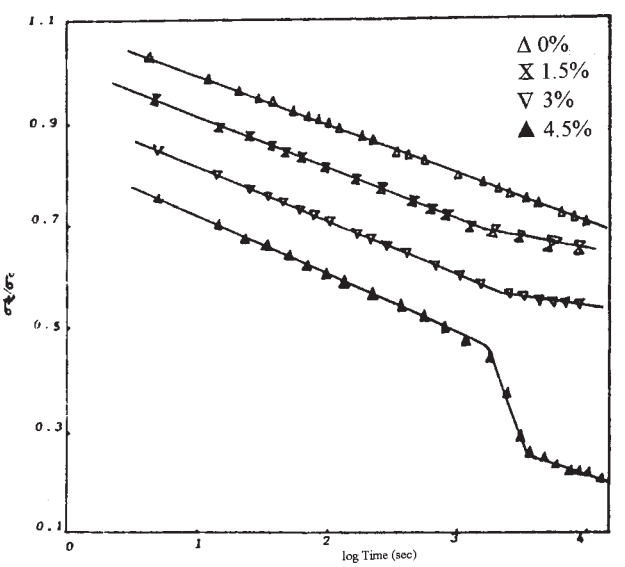

Figure 6 Effect of the compatibilizer loading on the stress-relaxation patterns of the 50/50 NR/PS blends: (△) 0, (×) 1.5, (▽) 3, and (▲) 4.5% graft copolymers.

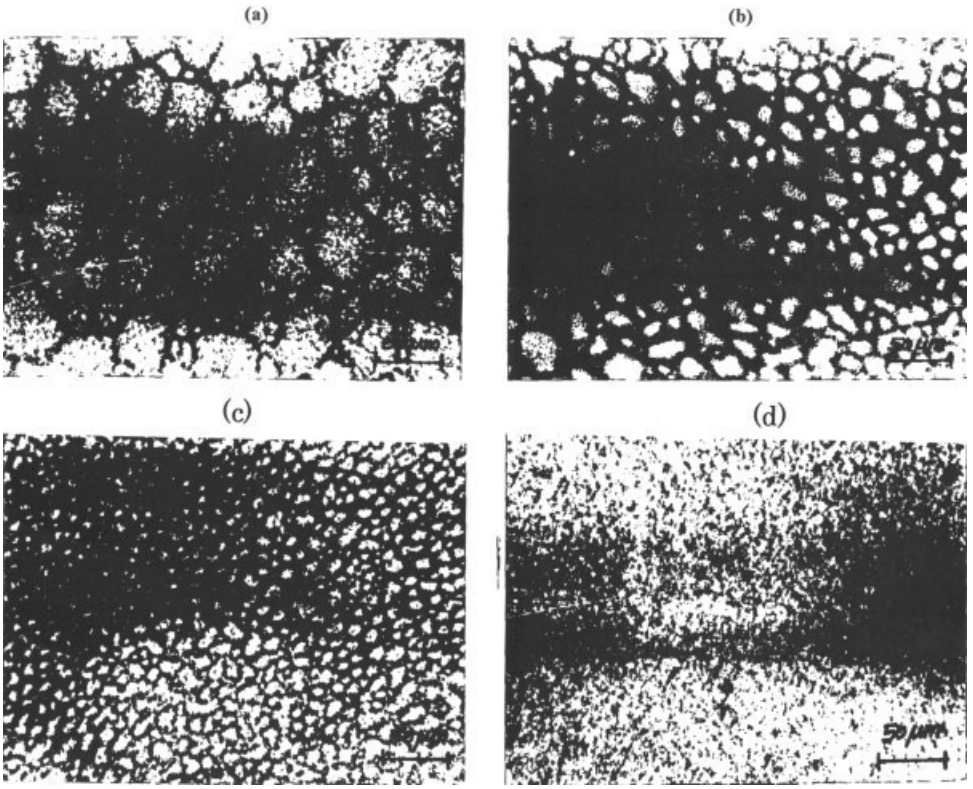

Figure 7 Optical micrographs of the 50/50 NR/PS blend with the (a) 0, (b) 1.5, (c) 3, and (d) 4.5% graft copolymers.

of micelle formation is highly undesirable. The cmc values were, in fact, estimated from the intersection of a straight line drawn at low concentration and the leveling off line at high concentration (Fig. 8). It is important to indicate that generally, the cmc value is estimated from the plot of interfacial tension versus copolymer concentration. Because the interfacial tension was directly proportional to the domain size,[16] the estimation of cmc from the plot of domain size versus concentration was justified.[5]

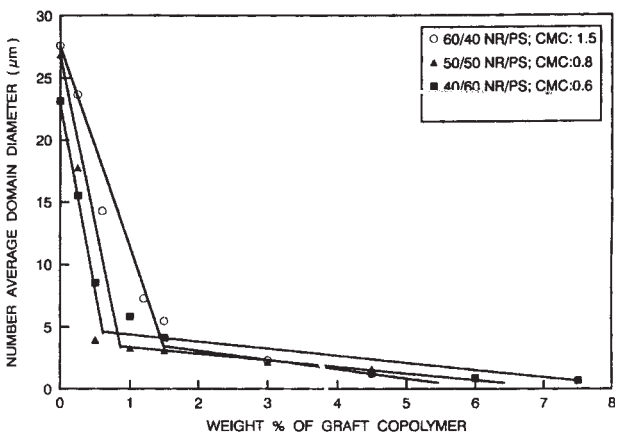

Figure 8 Effect of the copolymer concentration on the number-average domain diameter of the dispersed phase of different NR/PS blends.

Let us now look at the 50/50 blend in detail. Here, the leveling point (cmc) was found at 0.80% compatibilizer loading. The domain size of the blend without graft copolymer was 26.88 μm. The addition of 1.5% graft copolymer reduced the domain phase to 3.493 μm; that is, a reduction of 82.7% occurred. The addition of another 1.5% caused a reduction of 38% in the domain size. Finally, the domain size leveled off at higher concentrations. In the case of the 60/40 and 40/60 NR/PS blends, the percentages of graft copolymer required to saturate the interface (i.e., cmc) were 1.5 and 0.6%, respectively. This could be explained as follows. In the 60/40 NR/PS blend, NR formed a continuous phase, and PS formed the dispersed phase. The viscosity of the NR phase was much higher than that of the PS phase The graft polymer had to diffuse through the high-viscosity NR matrix to reach the interface. Because of the high viscosity of the NR phase compared to the PS phase, there were tremendous restrictions to the diffusion process. Therefore, all of the graft copolymers may not have reached the interface; as a result, some formed their own micellar aggregates. Therefore, one would have to add a larger quantity of the graft copolymer for interface saturation of this blend. On the other hand, in the 40/60 NR/PS blend, the low-

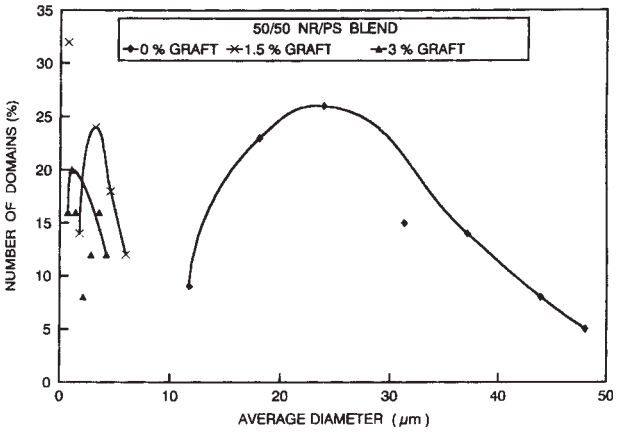

Figure 9 Effect of the copolymer concentration on the number-average domain size distribution of the 50/50 NR/PS blends.

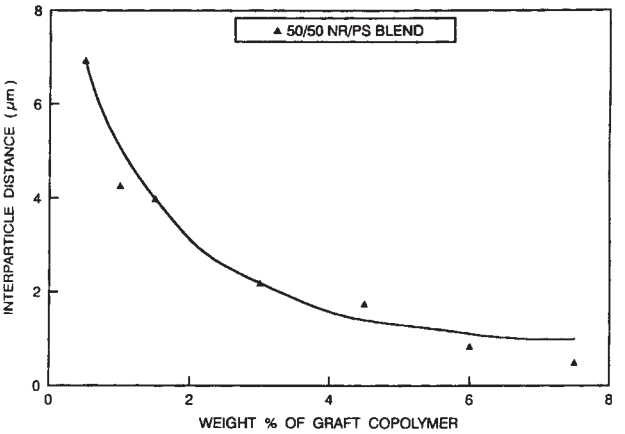

Figure 10 Effect of the copolymer concentration on the interparticle distance of the dispersed phase of the 50/50 NR/PS blend.

viscosity PS formed the matrix. Because of the low viscosity of the PS phase, the copolymer could easily diffuse toward the interface. Therefore, at lower concentrations of the graft copolymer, (0.6%) the interface got saturated in the 40/60 NR/PS blends.

The domain size distributions for the 50/50 NR/PS blend with and without the addition of the compatibilizer are given is Figure 9. Table V gives the standard deviation values of the blend (50/50) with and without the addition of the copolymer. These values decreased with increasing loading of the copolymer. The uncompatibilized blend contained large numbers of bigger particles. The PDI was higher for the blend without compatibilizer and was much reduced at higher concentrations of the compatibilizer, which was evident from the width of the distribution curve.

Figure 10 shows the effect of compatibilizer on the interparticle distance of dispersed domains in the 50/50 NR/PS blend system. The interparticle distance decreased with increasing concentration of the compatibilizer and finally leveled off at higher compatibilizer loadings. The compatibilizing action of NR-*g*-PS is schematically shown in Figure 11. Upon the addition of the compatibilizer (below cmc), the interfacial tension decreased, coalescence was suppressed, the dispersed phase size decreased, and the

TABLE V
Standard Deviation Values of the 50/50 NR/PS Blends

Percentage of the graft copolymer	Average domain size (μm)	Standard deviation
0.5	3.5	25.45
1	3.2	23.40
1.5	3.4	24.95
3	2.1	7.40
4.5	1.6	11.7
6	0.9	2.15

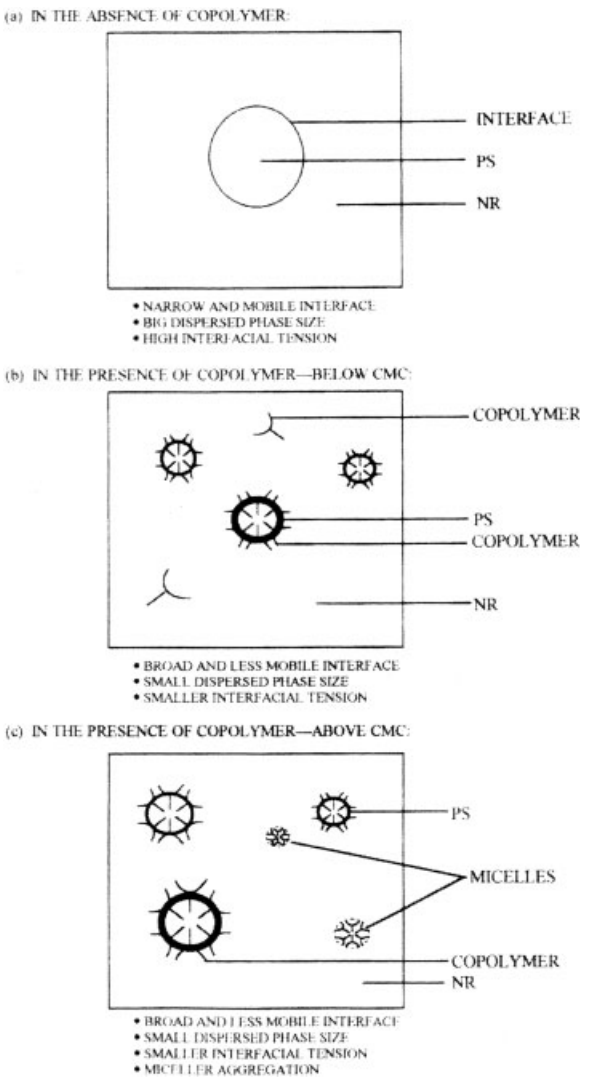

Figure 11 Schematic representation of the morphologies in the absence and presence of a compatibilizer (copolymer).

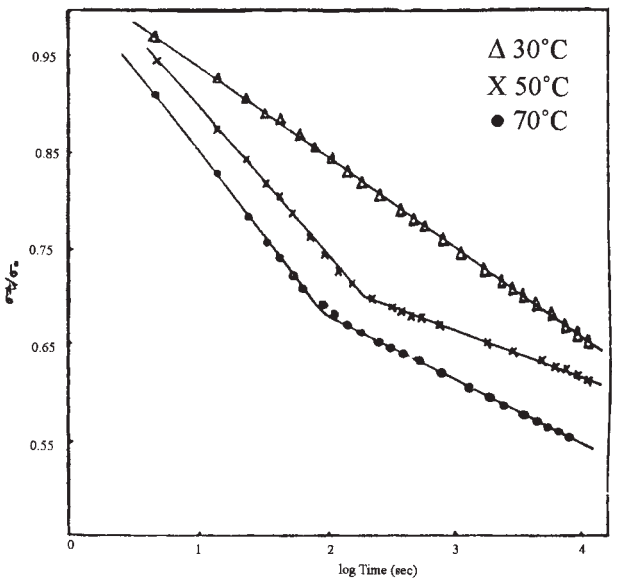

Figure 12 Effect of aging on the stress-relaxation pattern of the 50/50 NR/PS blends: (△) 30, (×) 50, and (●) 70°C.

interface became less mobile. However, above cmc, the copolymer formed micellar aggregation in the continuous phase. This micelle aggregation was responsible for the three-step mechanism observed in the relaxation process at high concentrations of the graft copolymer.

Effect of aging

To study the effect of aging, relaxation measurements were made with samples subjected to aging at 50 and 70°C for 4 days. The dependence of relative stress on log t is shown in Figure 12. In the case of the unaged 50/50 NR/PS blend, a single relaxation mechanism operated, whereas in the case of the aged samples, a two-stage mechanism was observed (i.e., samples G and H). The two-stage relaxation was associated with the transformation of the blend morphology from a cocontinuous morphology to a dispersed/matrix morphology. It is well known that phase coarsening occurs upon high-temperature annealing. In the case of the 50/50 NR/PS blends, we had a cocontinuous interpenetrating-network-like morphology. There was strong physical interaction between the NR and PS phases due to this interpenetration. Because of the interpenetrating-network-like morphology, the system showed a single relaxation mechanism. However, upon annealing at higher temperatures, the morphology was transformed to a dispersed/matrix phase morphology. In such morphologies, the interfacial interactions are extremely poor. Therefore, the system showed a two-stage mechanism.

The rates of relaxation for the aged and unaged samples are shown in Table III. In the case of aged samples, the rate of relaxation was high in the initial stage compared to later stages. In the aged samples, the initial increase in relaxation rate was due to the degradation of the rubbery phase. The later stages of relaxation were due to the plastic phase. The slopes and intercepts of these different stages are given in Table III and show that aging produced interesting effects on the stress-relaxation of these blends. The variation of slope at different stages of relaxation was gradual both at 50 and 70°C. The slope value indicated that the rate of relaxation was higher for the sample aged at 70°C compared to that aged at 50°C. In the case of sample G, the crossover time was lower (87 s) compared to that of sample H (171 s), and this was because the former case the matrix phase underwent degradation at a faster rate compared to the latter one.

CONCLUSIONS

The stress-relaxation behavior of various NR/PS blends in tension was studied with special reference to the effect of strain level, aging, composition, and compatibilizer loading. The relaxation patterns of different blends depended on the NR content and phase morphology. The cocontinuos morphology showed a single relaxation mechanism, whereas the dispersed/matrix phase morphology showed a two-step mechanism. The compatibilized blends showed a different pattern of relaxation compared to the noncompatibilized blends. The compatibilized blends below cmc followed a two-stage relaxation pattern, whereas above cmc, the blends followed a three-stage relaxation pattern that was associated with micelle formation. The compatibilized blends showed an increase in the rate of relaxation because of the presence of a boarder interface and improved interfacial interaction. Aging produced interesting effects on the relaxation pattern. Aged samples followed a two-stage relaxation pattern.

The authors are thankful to Siby Varghese, Scientist, Rubber Research Institute of India, Kerala, for his valuable help during this work.

References

1. Tucker C. L., III; Moldenaers, P. Annu Rev Fluid Mech 2002, 34, 177.
2. Patel, M.; Soames, M.; Skinner, A. R.; Stephens, T. S. Polym Degrad Stab 2004, 83, 111.
3. George, J.; Neelakandan, N. R.; Varughese, K. T.; Thomas, S. Rubber Chem Technol 2005, 78, 286.

4. Joseph, S.; Laupretre, F.; Negrell, C.; Thomas, S. Polymer 2005, 46, 9385.
5. Asaletha, R.; Kumaran, M. G.; Thomas, S. Rubber Chem Technol 1995, 68, 671.
6. Jansseune, T.; Vinckier, I.; Moldenaers, P.; Mewis, J. J Non-Newtonian Fluid Mech 2001, 99, 167.
7. Doi, M.; Ohta, T. J Chem Phys 1991, 95, 1242.
8. Maffettone, P. L.; Minale, M. J Non-Newtonian Fluid Mech 1998, 37, 227.
9. Cristini, V.; Macosko, C. W.; Jansseune, T. J Non-Newtonian Fluid Mech 2002, 105, 177.
10. Akinay, A. E.; Brostow, W.; Castano, V. M.; Maksimov, R.; Olszynski, P. Polymer 2002, 43, 3593.
11. Koga, J.; Kimura, K.; Homma, S. Chem Eng Sci 2007, 62, 2330.
12. Takahashi, M.; Macaúbasl, P. H. P.; Okamoto, K.; Jinnai, H.; Nishikawa, Y. Polymer 2007, 48, 2371.
13. Cooper, W.; Sewell, P. R.; Vanghan, G. J Polym Sci 1959, 41, 167.
14. Goni, M.; Chaga, G.; Sam Roman, J.; Valero, M.; Guzman, G. M. Polymer 1993, 34, 512.
15. Mackenzie, C. I.; Scanlan, J. Polymer 1984, 25, 559.
16. Wu, S. Polym Eng Sci 1987, 27, 335.